Proceedings World Geothermal Congress 2023
Beijing, China, April 17 – 21, 2023

Quantitatively investigate the effect of fracture roughness on hydraulic and electrical transport properties evolution induced by mineral dissolution

Yutian Zhang, Yuemiao Chen, Chengyong Li, Yinhui Zuo, Ziwei Wang

Institute of Industrial Technology, Chengdu University of Technology, Chengdu 610059, China

zhangyutian@cdut.edu.cn

Keywords: fracture, permeability, electrical conductivity, mineral dissolution, roughness

ABSTRACT

Monitoring the mineral dissolution process in rock fractures is very important at many subsurface systems, such as geothermal and carbon dioxide capture and storage projects. And transport properties of fractures are useful parameters to evaluate the underground reservoirs. Because the rock fracture is natural roughness, hence, understanding the role of roughness on the dissolution process is vital in geoengineering developments. However, the influence of roughness degree on transport properties evolution is rare quantitatively studied. To fill the research gap, herein, an adjusted-segment method is used to generate three artificial fracture models with various roughness, and the roughness degree is modeled by tortuosity. We applied a lattice Boltzmann method with dual multiple-relaxation-time (MRT) distribution functions to simulate the hydraulic transport property evolution in the mineral dissolution process in a wide range of Péclet (*Pe*) and Damköhler (*Da*) numbers. And the finite element method is employed to calculate the electrical conductivities of fracture models. The simulation results show that, the transport properties evolution is more sensitive to the Pe and Da numbers, rather than roughness. Finally, we proposed a model to predict the permeability from the electrical conductivity for a monitoring purpose.

1. INTRODUCTION

Mineral dissolution in fractured rocks extensively exists in many subsurface natural and engineering applications, such as geothermal exploration and development (Wu and Li, 2020), carbon geological sequestration with a mineralization approach (Snæbjörnsdóttir et al., 2020), and environmental contaminant remediation (Steefel et al., 2015). For example, From the viewpoint of engineering, being able to monitor the dissolution process is important for managing aquifers and reservoirs and for environmental studies because rock physical properties may change as a result of mineral dissolution and precipitation (Rembert et al., 2020; Kang et al., 2014).

Transport properties (i.e., hydraulic and electrical conductivities) of rocks are useful parameters to evaluate the reservoir on a field scale, however, their values are various on a pore scale (Hao et al., 2019). Therefore, understanding the evolution of transport properties induced by reactive transport in pore–scale is necessary. Mineral dissolution in fractured media is usually characterized by two dimensionless numbers, namely, Péclet and Damköhler numbers, many researchers have already experimentally and numerically investigated the dissolution mechanism in reservoir rocks (Kang et al., 2014; Ling et al., 2022). Most of these studies focused on reactive and hydraulic conditions effect, however, rare research quantitatively discussed the influence of fractures roughness on the reactive transport in pore scale.

In this work, we adjust Pe and Da numbers to remake different dissolution patterns in different fracture geometry models. A novel tortuosity parameter is proposed to characterize the roughness degree of fractures. A lattice Boltzmann method with dual multiple-relaxation-time (MRT) distribution functions is applied to simulate the reactive transport process in fractures. And finite element method with minimal energy is applied to simulate the electric current flow in the fractured matrix. We found that the permeability and electrical conductivity evolution curves present different trends, and both of them are controlled by roughness degree, reactivity, and hydraulic conditions. Finally, we propose a novel model to predict the permeability from electrical information considering the roughness influence.

2. MATERIALS AND METHODS

In this paper, we use artificial fractures with a segmented approach as the numerical experiment materials. A single-phase isothermal fluid flow model and single-solute mass transport model are integrated to explore the fracture roughness effect on the permeability and electrical conductivity evolution in mineral dissolution progress.

2.1 Materials

Natural fractures are commonly rough in underground formations. To mimic the roughness of single fracture, a segmented-linear approach (Shen et al., 2019) is used to reproduce the stochastic and roughness surfaces. The algorithm is explained as follows:

First step: The fracture surface projection along the horizontal direction is divided into unequal n finite segments, and each length of these segments can be expressed as

$$L_i = L_{Max} * \zeta, \tag{1}$$

where ζ is the coefficient in the range between (0,1), and L_{Max} is called the maximum length for each segment, its value affect the topology of the fracture surface.

Second step: Specify the start point height of the surface as h_0, and then, for the end point height of each segment, it is taken as

$$h_i = h_{max} * \delta, \tag{2}$$

δ is a random parameter in the range between (0,1), and h_{max} is called the maximum height for each end point. Both of L_{Max} and h_{max} together determine the roughness degree of the fracture surface.

Third step: Connecting the end to end for all segments, and the single surface of the roughness fracture is generated. After this, move the whole surface along the vertical direction with a distance d_0, which is equivalent to aperture.

Finally, a mated fracture with the aperture d_0 is produced. Totally, we adopt the h_{max} and with fixed L_{Max} and d_0, there are three two-phase (i.e., solid and fluid phases) fracture models are generated with $h_{max} = 0\ lu$, $h_{max} = 20\ lu$, and $h_{max} = 40\ lu$ can be found in Figure 1.

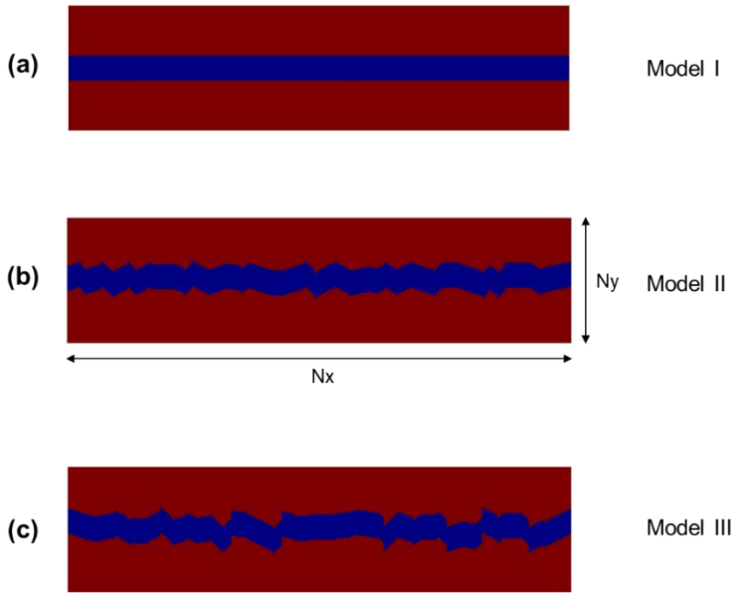


Figure 1. Three mated fractures with (a) $h_{max} = 0\ lu$, (b) $h_{max} = 20\ lu$, and (c) $h_{max} = 40\ lu$. And red color regions indicate solid phase, and blue color regions indicate fluid phase.

2.2 Mathematical models

2.2.1 Mathematical models for fluid flow and solute transport

For isothermal incompressible single-phase fluid flow in pore scale, Navier-Stokes and continuity equations are used to describe the phenomena as follows (Landau and Lifshitz, 1987; Krüger et al., 2017)

$$\nabla p = \mu \Delta \boldsymbol{u}, \tag{3}$$

$$\nabla \cdot \boldsymbol{u} = 0, \tag{4}$$

where p, μ, and $\boldsymbol{u}$ represent pressure, dynamic shear viscosity of fluid, and velocity vector, respectively.

For solute transport in fractures, advection–diffusion equation is considered as

$$\frac{\partial C}{\partial t} + \nabla \cdot (C\boldsymbol{u}) = \nabla \cdot (D \nabla C) \tag{5}$$

where C is the scalar quantity of solute concentration, and D is the diffusion coefficient of solute.

Mineral dissolution is considered as a heterogeneous reaction at solid surfaces. The chemical reaction process can be treated with a boundary condition as follows (Kang et al., 2014; Liu and Mostaghimi, 2017):

$$D \frac{\partial C}{\partial \boldsymbol{n}} = \hat{I} = k_r (C - C_{eq}), \tag{6}$$

where C_{eq} is the solute concentration in equilibrium status, $\hat{I}$ is the reactive flux due to surface kinetic reaction, and $\boldsymbol{n}$ is the direction normal from solid surface pointing toward the fluid phase. In this work, the isolated solid grains movement within fluid drag force is not considered, therefore, the stationary mineral volume update at each time step is given by (Kang et al., 2014)

$$\frac{\partial \phi_V}{\partial t} = \bar{V} a \hat{I}, \tag{7}$$

where $\bar{V}$ and a are the molar volume and specific area, respectively.

2.2.2 Darcy and Ohm laws in porous medium

At a low Reynold number ($\ll 1$), the viscosity fluid flow in a fractured medium experimentally conforms Darcy's law (Walsh and Brace, 1984):

$$Q = -\frac{KA}{\mu}\nabla p, \tag{8}$$

where Q is the volumetric flow rate, K is the hydraulic conductivity and A is the cross-sectional area of a fractured rock. Like to Darcy's law, the conduction of electrical current through a fractured medium saturated with an electrolyte follows the modified Ohm's law

$$I = -\frac{A}{F}\sigma_f \nabla v, \tag{9}$$

where I is the electrical current, F is the formation factor defined as the ratio of the fluid conductivity to the fractured rock with fluid filled, σ_f is the fluid electrical resistivity, and v is the voltage or electrical potential.

2.3 Numerical models

Contrasting conventional computational fluid dynamic methods (e.g., finite difference, finite volume) that directly solve the governing equations (Eq. 3 and 4), the LB method discretizes the Boltzmann equation (Krüger et al., 2017; Guo and Shu, 2013) to approximately obtain the solutions of these governing equations. Due to the simplicity and efficiency of LB model, it has already attracted many interest in industry and academic. Considering the stability and accuracy of the relation time model, a population evolution equation with multiple-relation-time (MRT) model is selected as (Krüger et al., 2017; Luo et al, 2011):

$$f_i(\boldsymbol{x} + \boldsymbol{c}_i\Delta t, t + \Delta t) - f_i(\boldsymbol{x}, t) = -\boldsymbol{M}^{-1}\boldsymbol{S}_f\boldsymbol{M}[f_i(\boldsymbol{x}, t) - f_i^{eq}(\boldsymbol{x}, t)], \tag{10}$$

$$f_i^{eq}(\boldsymbol{x}, t) = \omega_i\rho(1 + \frac{\boldsymbol{u}\cdot\boldsymbol{c}_i}{c_s^2} + \frac{(\boldsymbol{u}\cdot\boldsymbol{c}_i)^2}{2c_s^4} - \frac{\boldsymbol{u}\cdot\boldsymbol{u}}{2c_s^2}), \tag{11}$$

where f_i is the population along the i–direction, $\boldsymbol{c}_i$ is the discrete micro-velocity, and the D2Q9 micro velocity model is applied; f_i^{eq} is the equilibrium population, and $\boldsymbol{M}$ is the transformation matrix given by Eq. 12; $\boldsymbol{S}_f$ is the relaxation time matrix in Eq. 13, and ω_i is the weight parameter. The fluid density and velocity are given by $\rho = \sum f_i$ and $\rho\boldsymbol{u} = \sum f_i\,\boldsymbol{c}_i$, respectively. c_s is the sound speed expressed as $c_s^2 = 1/3$ with the D2Q9 model, where Δt is the time step, and Δx is the size of the lattice grid.

$$\boldsymbol{M} = \begin{bmatrix} 1 & 1 & 1 & 1 & 1 & 1 & 1 & 1 & 1 \\ -4 & -1 & -1 & -1 & -1 & 2 & 2 & 2 & 2 \\ 4 & -2 & -2 & -2 & -2 & 1 & 1 & 1 & 1 \\ 0 & 1 & 0 & -1 & 0 & 1 & -1 & -1 & 1 \\ 0 & -2 & 0 & 2 & 0 & 1 & -1 & -1 & 1 \\ 0 & 0 & 1 & 0 & -1 & 1 & 1 & -1 & -1 \\ 0 & 0 & -2 & 0 & 2 & 1 & 1 & -1 & -1 \\ 0 & 1 & -1 & 1 & -1 & 0 & 0 & 0 & 0 \\ 0 & 0 & 0 & 0 & 0 & 1 & -1 & 1 & -1 \end{bmatrix} \tag{12}$$

$$\boldsymbol{S}_f = diag\big(0, s_e, s_\epsilon, 0, s_q, 0, s_q, s_v, s_v\big) \tag{13}$$

In Eq. (2.20), s_e and s_v are related by the bulk viscosity (v) and shear viscosity (ζ) described as follows:

$$v = \frac{1}{3}\left(\frac{1}{s_v} - \frac{1}{2}\right)\Delta x^2/\Delta t, \tag{14}$$

$$\zeta = \frac{1}{3}(\frac{1}{s_e} - \frac{1}{2})\Delta x^2/\Delta t. \tag{15}$$

The s_ϵ and s_q are free parameters that can be tuned for good numerical accuracy and stability (Luo et al., 2011).

LB model also can recover the advection-diffusion equation (ADE) (Krüger et al., 2017; Sullivan et al., 2005), in this paper, a MRT model for ADE is also adopted to reach more accuracy and stability, which can be formulated as

$$g_i(\boldsymbol{x} + \boldsymbol{c}_i\Delta t, t + \Delta t) - g_i(\boldsymbol{x}, t) = -\boldsymbol{M}^{-1}\boldsymbol{S}_c\boldsymbol{M}[g_i(\boldsymbol{x}, t) - g_i^{eq}(\boldsymbol{x}, t)], \tag{16}$$

$$g_i^{eq}(\boldsymbol{x}, t) = \omega_i C(1 + \frac{\boldsymbol{u}\cdot\boldsymbol{c}_i}{c_s^2} + \frac{(\boldsymbol{u}\cdot\boldsymbol{c}_i)^2}{2c_s^4} - \frac{\boldsymbol{u}\cdot\boldsymbol{u}}{2c_s^2}), \tag{17}$$

where the solute concentration C is given by $C = \sum g_i$, and the diagonal relaxation matrices $\boldsymbol{S}_c$ of relaxation rates are given by

$$\boldsymbol{S}_c = diag(s_0, s_1, s_2, s_3, s_4, s_5, s_6, s_7, s_8), \tag{18}$$

and the selection of relation rate parameters follows Meng and Guo, (2015). A boundary condition is applied for treating the surface reaction (Kang, et al., 2002, 2006).

To mimic the electrical current flow in the porous media, the finite element method with minimal energy approach is employed in this study. The details can be found in Garboczi (1999).

3. RESULTS AND DISCUSSIONS

Mineral dissolution in roughness fractures were numerically explored applying Lattice Boltzmann method. The kinetic chemical reaction is considered as

$$A(aq) + B(s) \longrightarrow C(aq) \tag{19}$$

which means that, at the initial state, the solute concentration is zero. As the solvent is injected from the inlet, once the acid solution contacts the solid phase, the mineral dissolution progress started. It is noted that, because the dissolution reaction is considered irreversible, therefore the solute C(aq) influence is ignored. When the dissolution occurs, the porosity and permeability of fractured rock alter gradually. In regard to the treatment of boundary conditions, the no-slip is imposed for fluid and solute at the upper and bottom; pressure boundaries are used at the inlet and outlet for fluid flow; constant concentration boundary is applied at the inlet for the solute, and zero-diffusion gradient boundary is applied at the outlet for the solute. And for the solid-fluid interface, the half-way bounce-back is employed. A mesh of size $N_x * N_y = 400 * 100\ lu^2$ is selected, Wennberg, et al., (2019) reported that the average aperture of natural fractures in the subsurface is 183 μm, hence, the resolution of spatial scale is 9.15 $\mu m/lu$.

In our simulations, the permeability is expressed as $k = u_D \rho \nu L/(p_i - p_o)$ (Kang et al., 2002, 2014), where u_D is the Darcy velocity calculated by averaging the velocity along the main flow direction over the entire region. L is the length of the computational domain, and p_i and p_o are the inlet pressure and outlet pressure, respectively. Here, Pe and Da can be calculated as $Pe = u_D H/D$ and $Da = k_r Nx/D$. 48 simulations for a range of Pe {10^{-2}, 10^{-1}, 10^{0}, 10^{1}}and Da {10^{-2}, 10^{-1}, 10^{0}, 10^{1}} were conducted on the three fracture models.

To characterize the roughness degree in different fracture models, we propose a novel parameter effective tortuosity τ_n, which is given by

$$\tau_n = (\tau_h + \tau_e)/2 \tag{20}$$

where τ_h and τ_e are hydraulic and electrical tortuosity, respectively. And the two tortuosity is computed as (Duda et al. 2008)

$$\tau_i = \frac{\langle v \rangle}{\langle v_x \rangle}, i = h, e \tag{21}$$

where $\langle v \rangle$ represents the integral of velocity or current magnitude in the pore space, and $\langle v_x \rangle$ represents the integral of the velocity or current magnitude along the major flow directions in the pore space. The results of three fracture models are 1.0005, 1.0129, and 1.0288 corresponding to model I, model II, and model III (see Fig. 1), respectively.

3.1 Roughness influence on permeability

In this work, we adjust *Pe* and *Da* numbers to reproduce various mineral dissolution regimes in fractured rocks. There are three typical dissolution patterns, uniform, face and wormhole dissolutions were detected in these three fractures (see Fig. 2) corresponding to {*Pe*=10, *Da*=0.01}, {*Pe*=0.01, *Da*=10}, and {*Pe*=10, *Da*=10} at model III, model II, and model I, respectively. And other dissolution regimes are hybrid coupled by three dissolution regimes under various *Pe* and *Da* conditions.

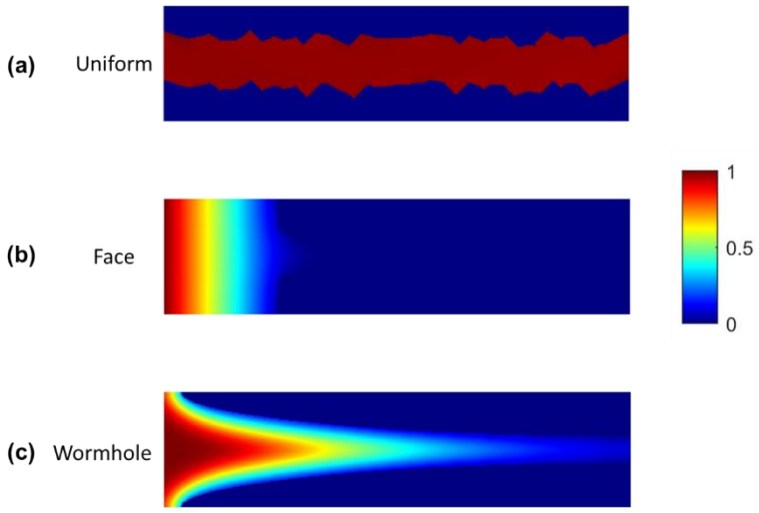


Figure 2. Solute concentration profiles of three typical dissolution patterns in fractured rocks. (a): uniform dissolution at *Pe*=10, *Da*=0.01 in model III, (b): face dissolution at *Pe*=0.01, *Da*=10 in model II, and (c): wormhole dissolution at *Pe*=10, *Da*=10 in model I.

Because different dissolution regimes carve different topology profiles of roughness fracture, thus, the permeability alterations in different Pe and Da conditions are also varied. The normalized porosity–permeability relationships with a wide range of Pe and Da conditions with three fractured mediums can be found in Figure 3. We can find that, porosity–permeability curves trends are similar at identical Pe and Da conditions in different fractured rocks, however, the increase rates in different roughness fracture models are dramatically different, it can be observed that, under identical hydraulic and reactive conditions, the roughness degree larger, the evolution rate of permeability faster. And in Fig. 3, especially, as the black arrows are shown in Fig 3(b) and (c), at more roughness fracture models, when Pe=10 and Da=10, their trends obviously differ. This is because the pore space becomes more heterogeneous at the more roughness fractures, which leads to the solute transport being more dispersive, and therefore, the permeability alteration rate is accelerated.

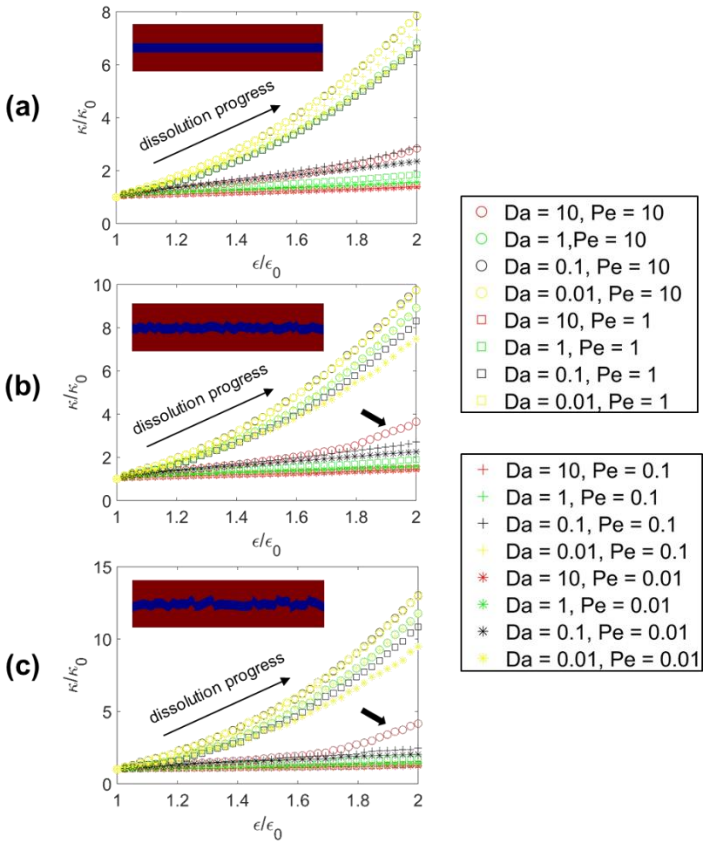


Figure 3. Normalized porosity and permeability relationships with various Pe and Da conditions at (a) 1.0005, (b) 1.0129, and (c) 1.0288.

3.2 Roughness influence on electrical conductivity

The results of variation of electrical conductivity in three fractured models with a wide range of Pe and Da conditions are shown in Fig. 4. The normalized porosity–electrical conductivity curves exhibit similar trends in different fracture mediums, it can be observed that, under the same Pe and Da conditions, when the roughness degree becomes larger, the evolution rate of electrical conductivity become faster. The phenomena also can be explained that the more heterogeneous fluid phase space induces to solute transport be more dispersive, therefore accelerating the electrical conductivity change rate. However, there are several differences between permeability and electrical conductivity evolution trends under identical Pe and Da numbers in the same fracture model. It is because that fluid flow cannot penetrate the solid surface whereas the electrical current is able to pass through the fluid-solid interface (see Fig. 5), and hence, their flow distributions are different (see Fig. 5a and b).

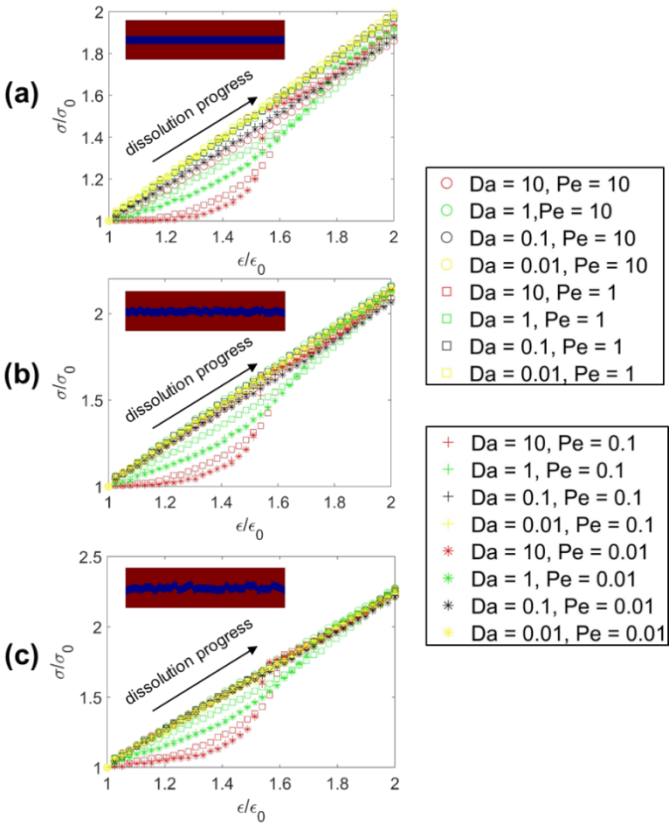


Figure 4. Normalized porosity and electrical conductivity relationships with various Pe and Da conditions at (a): Model I, (b): Model II, and (c): Model III.

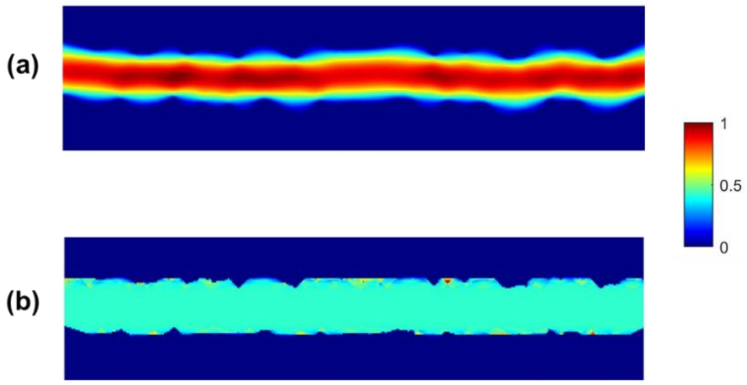


Figure 5. Examples of normalized (a) velocity and (b) electrical current magnitude profiles when Pe=10 and Da=0.01 in the fracture model with effective tortuosity equals to 1.0288.

3.3 Prediction model for permeability through electrical conductivity

In geo-energy engineering projects, for dynamic monitoring hydraulic conductivity with low cost, a model which can be used to predict permeability from well data is expected. Commonly, the plot of formation factor against permeability was used to study the relationship between permeability and electrical conductivity. And as shown in Fig. 3 and 4, the permeability and electrical conductivity evolution trends are roughly similar, hence, we construct a model to predict permeability evolution under various hydraulic and reactive conditions in fracture models in the dissolution process as shown in Fig. 6. We can find that corresponding to high Pe and high Da conditions (i.e., >=1), there are apparently two segments linear relationships (i.e., red and green symbols representation cases) emerge in roughness models. And as the fracture becomes rougher, the transition point from one linear to another linear relationship is earlier (see black arrows in Fig. 6), which is because, when Pe and Da are both high, the mineral dissolution in fractures are wormhole regimes, and as the surface profiles of fracture become more roughness, dissolution processes more easily smooth the corners and edges of the roughness surfaces, therefore the transition point occurs earlier in Fig. 6b and c. And for other Pe and Da conditions, linear relationships are observed.

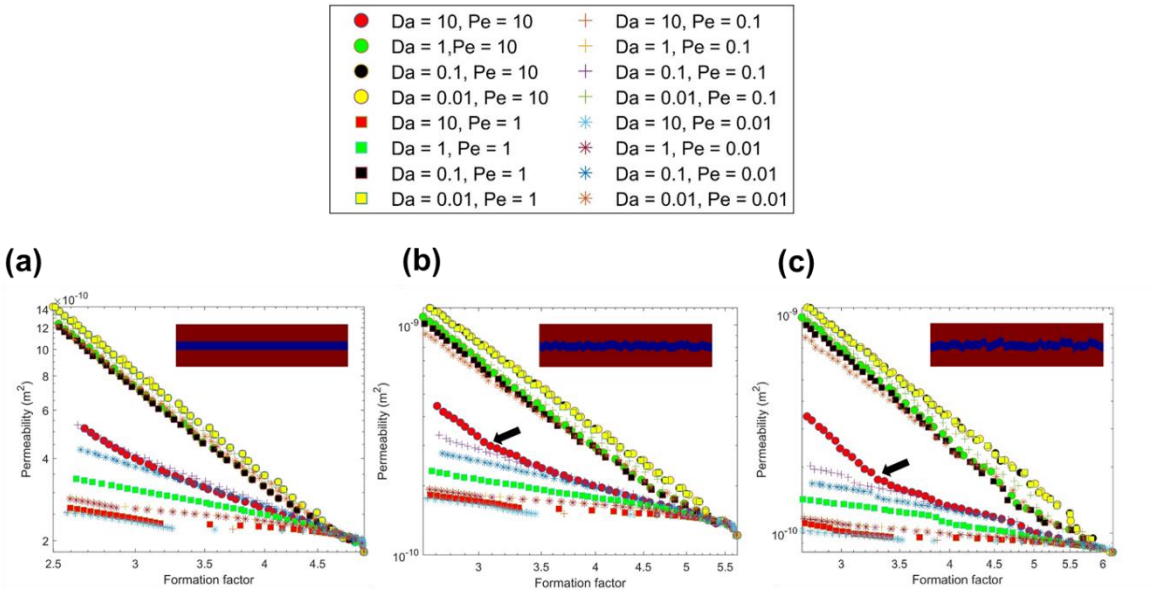


Figure 6. Formation factors against permeability in three roughness fractures related to (a) 1.0005, (b) 1.0129, and (c) 1.0288.

4.APPLICATION

Our results reveal that permeability alteration rate and dissolution patterns of minerals vary in different fracture reservoir rocks under same chemical and hydraulic conditions. In carbon dioxide capture and storage projects, it is important to monitor the mineral dissolution process in rock fractures and rock permeability in many underground systems. By understanding the mineral dissolution process in rock fractures and the law of permeability evolution, the ideal "*Carbon Pool*" can be identified and its storage performance can be evaluated, including storage difficulty, storage capacity and sealing performance.

In geothermal projects, the proposed permeability prediction model can be used to monitor the hydraulic conductivity combining with well data at a low cost. The evolution trends of permeability and conductivity are roughly similar, corresponding to the conditions of high Pe and high Da (i.e., >=1), and two linear relationships appear obviously in the roughness model in fig.6. The rougher the crack, the earlier the transition point from one linear relationship to the other, because when Pe and Da are both high, the minerals in the crack dissolve into wormhole states, and the rougher the crack surface profile, the easier the dissolution process is to smooth the edges and corners of the rough surface.

Geothermal development and recharge will cause the temperature and pressure of thermal reservoir to be permeated, and the chemical balance between formation water and reservoir rocks will be destroyed, which may lead to the dissolution or precipitation of minerals in rocks due to temperature changes, and the dissolution or precipitation of mineral components may lead to the change of reservoir permeability by changing pore space geometry and pore connectivity. Especially when the water temperature is high and 100 ℃, the reaction rate increases exponentially with temperature, and the permeability changes are more significant and complex. On the one hand, the efficiency of thermal storage and irrigation is reduced, and on the other hand, the reservoir structure is damaged (Huang et al., 2020).

5. CONCLUSIONS

In this paper, we applied the lattice Boltzmann method and finite element method to mimic the mineral dissolution process and electrical current flow in fractured rocks, respectively. A segmented-linear approach is used to generate three roughness fractures for a quantitative investigation purpose. A novel parameter is proposed to characterize the roughness degree for fracture models. We found that permeability and electrical conductivity evolution rates are faster in more rough fractured structures. And a model for predicting permeability from electrical information is suggested.

REFERENCES

[1] Garboczi, E.J., 1998. Finite element and finite difference programs for computing the linear electric and elastic properties of digital image of random materials. Natl Inst Stand Technol Interag Rep 6269.

[2] Hao, Y., Smith, M. M., & Carroll, S. A. (2019). Multiscale modeling of CO2-induced carbonate dissolution: From core to meter scale. International Journal of Greenhouse Gas Control, 88(June), 272–289.

[3] Kang, Q., Chen, L., Valocchi, A.J., Viswanathan, H.S., 2014. Pore-scale study of dissolution-induced changes in permeability and porosity of porous media. J. Hydrol. 517, 1049–1055. https://doi.org/10.1016/j.jhydrol.2014.06.045

[4] Kang, Q., Lichtner, P. C., & Zhang, D. (2006). Lattice Boltzmann pore-scale model for multicomponent reactive transport in porous media. Journal of Geophysical Research: Solid Earth, 111(5), 1–12.

[5] Kang, Q., Zhang, D., Chen, S., & He, X. (2002). Lattice Boltzmann simulation of chemical dissolution in porous media. Physical Review E - Statistical Physics, Plasmas, Fluids, and Related Interdisciplinary Topics, 65(3).

[6] Krüger, T., Kusumaatmaja, H., Kuzmin, A., Shardt, O., Silva, G., Viggen, E.M., 2017. The Lattice Boltzmann Method. https://doi.org/10.1007/978-3-319-44649-3

[7] L.D. Landau, E.M. Lifshitz, Fluid Mechanics (Pergamon Press, Oxford, 1987)

[8] Ling, B., Sodwatana, M., Kohli, A., Ross, C. M., Jew, A., Kovscek, A. R., & Battiato, I. (2022). Probing multiscale dissolution dynamics in natural rocks through microfluidics and compositional analysis. *Proceedings of the National Academy of Sciences of the United States of America*, *119*(32), e2122520119. https://doi.org/10.1073/pnas.2122520119

[9] Liu, M., Mostaghimi, P., 2017. Characterisation of reactive transport in pore-scale correlated porous media. Chem. Eng. Sci. 173, 121–130. https://doi.org/10.1016/j.ces.2017.06.044

[10] Luo, L.S., Liao, W., Chen, X., Peng, Y., Zhang, W., 2011. Numerics of the lattice Boltzmann method: Effects of collision models on the lattice Boltzmann simulations. Phys. Rev. E - Stat. Nonlinear, Soft Matter Phys. 83, 1–24. https://doi.org/10.1103/PhysRevE.83.056710

[11] Meng, X., & Guo, Z. (2015). Multiple-relaxation-time lattice Boltzmann model for incompressible miscible flow with large viscosity ratio and high Péclet number. *Physical Review E - Statistical, Nonlinear, and Soft Matter Physics*, *92*(4). https://doi.org/10.1103/PhysRevE.92.043305

[12] Petter Wennberg Equinor ASA, O., Naumann Equinor ASA, M., Jonoud, S., & Yu Rozhko Equinor ASA, A. (n.d.). *Fracture aperture in reservoir rocks: examples from the Shetland Chalk in the Gullfaks Field Carbonates-impact of fractures on Hydrocarbon Production View project Fluid flow across fracture-matrix interfaces in fractured carbonates View project*. https://www.researchgate.net/publication/331563274

[13] Rembert, F., Jougnot, D., Guarracino, L., 2020. A fractal model for the electrical conductivity of water-saturated porous media during mineral precipitation-dissolution processes. Adv. Water Resour. 145, 103742. https://doi.org/10.1016/j.advwatres.2020.103742

[14] Snæbjörnsdóttir, S. Ó., Sigfússon, B., Marieni, C., Goldberg, D., Gislason, S. R., & Oelkers, E. H. (2020). Carbon dioxide storage through mineral carbonation. Nature Reviews Earth & Environment, 1(2), 90–102.

[15] Steefel, C. I., Appelo, C. A. J., Arora, B., Jacques, D., Kalbacher, T., Kolditz, O., … Yeh, G. T. (2015). Reactive transport codes for subsurface environmental simulation. Computational Geosciences (Vol. 19).

[16] Sullivan, S.P., Sani, F.M., Johns, M.L., Gladden, L.F., 2005. Simulation of packed bed reactors using lattice Boltzmann methods. Chem. Eng. Sci. 60, 3405–3418. https://doi.org/10.1016/j.ces.2005.01.038

[17] Walsh, J.B., Brace, W.F., 1984. The effect of pressure on porosity and the transport properties of rock. J. Geophys. Res. 89, 9425–9431. https://doi.org/10.1029/JB089iB11p09425

[18] Wu, Y., Li, P. The potential of coupled carbon storage and geothermal extraction in a CO2-enhanced geothermal system: a review. Geotherm Energy 8, 19 (2020). https://doi.org/10.1186/s40517-020-00173-w

[19] Z. L. Guo and C. Shu, Lattice Boltzmann Method and its Applications in Engineering World Scientific Publishing, Singapore, 2013. http://dx.doi.org/10.1142/8806

[20] L.F.Shen,Z.L.Wang,Y.Zeng,Z.Li&S.J.Li.(2019).A coupled seepage and dissolution model of rough rock fractures considering surface reaction based on lattice Boltzmann method,Chinese Journal of Rock Mechanics and Engineering(08),1615-1626. doi:10.13722/j.cnki.jrme.2019.0194

[21] Y.H.Huang,L.H.Wu,B.Bai,Y.X.Cui,R.C.Lu,Z.H.Pang,Multi-field coupling simulation technology and its application in safety evaluation of geothermal exploitation,Innovation in China,2020,Volume 16, Issues 3-4,323-331.